Colloid Polym Sci (2007) 285:405–411
DOI 10.1007/s00396-006-1572-x

ORIGINAL CONTRIBUTION

The relationship of conductivity to the morphology and crystallinity of polyaniline controlled by water content via reverse microemulsion

Qiong Zhou · Jiewei Wang · Yuliang Ma · Chuanbo Cong · Fang Wang

Received: 25 May 2005 / Accepted: 3 December 2005 / Published online: 15 November 2006
© Springer-Verlag 2006

Abstract Conducting polyaniline (PANI) with the controllable morphology and crystallinity were successfully synthesized with different water content ($W_0 = [H_2O]/[AOT]$) in the reverse microemulsion stabilized with sodium bis(2-ethylhexyl)-sulfosuccinate (AOT). In the microemulsion, the systems containing the different amounts of water will show the different phase behaviors and structures. The influence of water content on morphology and crystallinity of conducting PANI was characterized by a number of techniques such as Fourier transform infrared spectra, UV–Visible, scanning electron microscopy, transmission electron microscopy, and X-ray powder diffraction and conductivity. In particular, we focus on the understanding of the relationship between the morphology and the crystallinity and the conductivity of PANI powder. With the increasing of the water content (W_0=13.9, 27.8, 55.5, and 111.1) in the microemulsion system, the morphology and the crystallinity obviously changed and the values of relative conductivity are 0.05, 0.11, 2.7, and 1.8 S/cm, respectively.

Keywords Reverse microemulsion · Polyaniline (PANI) · Sodium bis(2-ethylhexyl)-sulfosuccinate (AOT) · Water content

Introduction

Polyaniline (PANI) is one of the most studied conducting polymers in the past 20 years [1], which is conventionally synthesized by chemical or electrochemical method [2, 3]. In accord with early works, various kinds of dopants [4, 5] were studied to improve its conductivity and processability. At the same time the different polymerization methods were examined, such as solution polymerization, reverse microemulsion polymerization [6–9], and dispersion polymerization [10, 11]. In solution polymerization, the researchers can hardly control the morphology of PANI. On the other hand, PANI particles of spherical, rice-grain, or needle-like morphology of varying polydispersity in size were synthesized by steric stabilizer [12], but it is hard to analyze the component of compound and the configuration of PANI. Reverse microemulsion is of special interest not only because a variety of reactants can be introduced into the nanometer-sized aqueous domains to control the size and shape of materials [13], but also because higher crystallinity PANI can be synthesized in reverse microemulsions. In recent years, a majority of studies were focused on morphology [14], crystallinity [15], and electrical properties. Some researchers have found that the morphologies of PANI have a significant dependence on the kinds of the dopants and the synthesized methods [16], and the conductivity also strongly depends on the degree of crystallinity [17].

Conductivity is a very important property of PANI and it was intensively studied by many research groups. First, the structure of chain influences the electrical property: The PANI doped with protonic acids can form intermediate oxidation state (the protonated emeraldine). Protonation induces an insulator-to-conductor transition. Second, it is believed that the interchain electron mobility in a given polymer is significantly increased with ordered solid state structure such as crystalline domains, which can improve interchain electron coupling [18]. Thus, another method of achieving a higher level of conductivity in PANI is to

Q. Zhou (✉) · J. Wang · Y. Ma · C. Cong · F. Wang
Department of Materials Science and Engineering,
China University of Petroleum,
Beijing 102249, People's Republic of China
e-mail: zhouqiong_cn@163.com

induce crystallinity [19]. Besides, PANI progressively increased in crystallinity after doping with aqueous HCl, and remarkably increased in conductivity. As described above, each conducting polymer particle can be considered as a crystal grain, and every crystal grain is a conductor so the degree of crystallization is more perfect, and the electric conductivity rate is higher. And the particles polymerized in the various-sized spaces may get different crystallinities. Therefore, the size of crystal grain and the degree of crystallinity dramatically affect the conductivity.

Using the microemulsion as a reaction medium, we can control the size of microemulsion droplet and work on the characteristics of PANI. A convenient way to control the size of polymerization place is at a fixed surfactant concentration, so the water content ($W_0 = [H_2O]/[AOT]$) can then be employed. The changes of water content induce the morphology change of surfactant aggregates in respective systems [20, 21]. To investigate the phase behavior and the structure of microemulsion, electrical conductivity (curve of W_0 changed with the solution electrical conductivity) is performed [22]. Electrical conductivity illustrates the degree of percolation or the bicontinuous nature of a microemulsion system. In our experiment, ionic surfactants Aerosol–OT (AOT) was used because of its ability to formulate reverse micelles containing large amounts of water without the addition of a cosurfactant [23, 24]. Pitchumani et al. [24] have prepared nanoparticles of PANI in AOT micelles. They found that the polymer exhibited a well-defined crystalline phase, which was orthorhombic [25]. But in their study, they used excessive surfactant and did not report the morphology of PANI.

In the present study, we prepared PANI in AOT reverse microemulsion and discussed the relationship between the morphology, crystallinity, and electroconducting behavior with the changes of W_0.

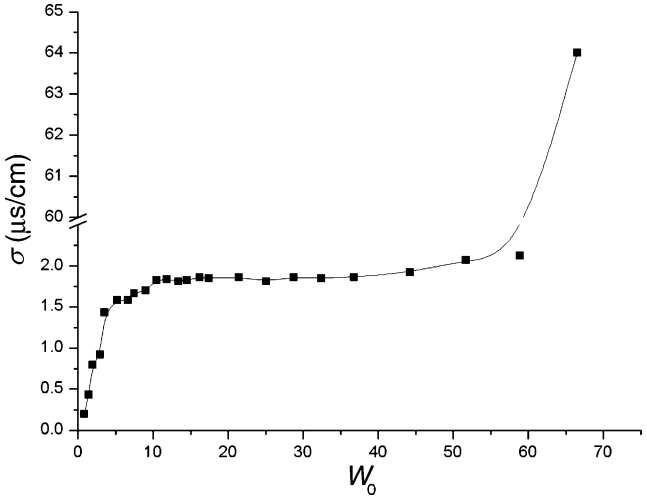

Fig. 1 Variation of electrical conductivity as function of water content in AOT microemulsion

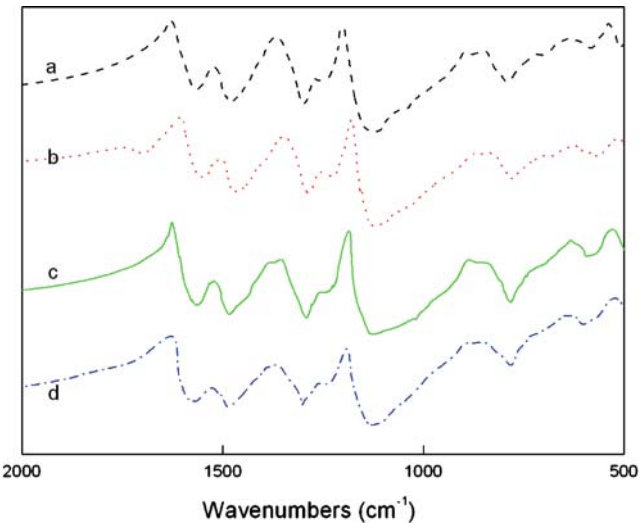

Fig. 2 FT-IR spectra of PANI synthesized by different water content AOT microemulsion: **a** W_0=13.9, **b** W_0=27.8, **c** W_0=55.5, and **d** W_0=111.1

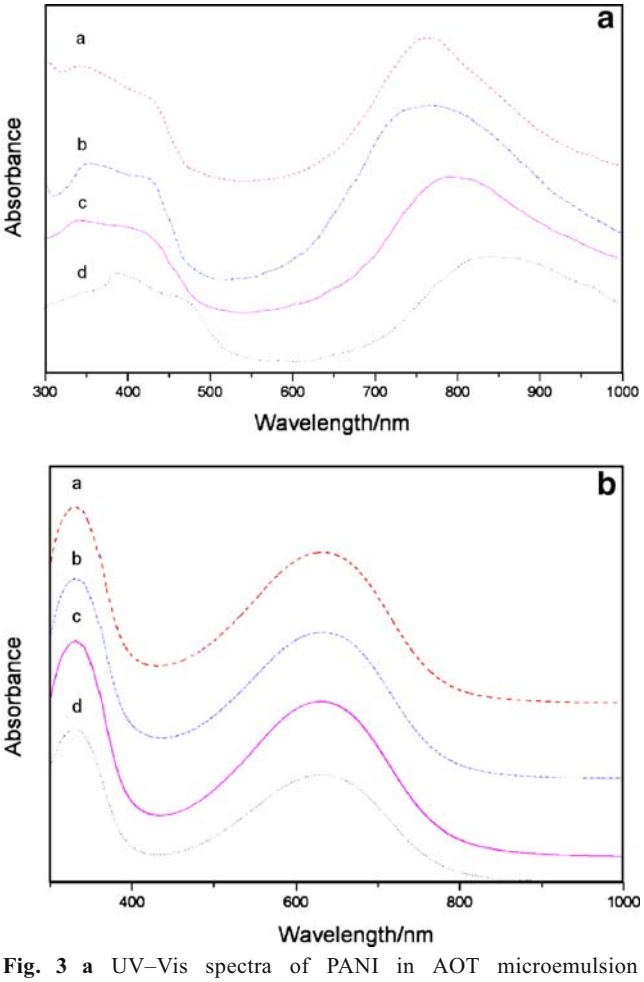

Fig. 3 **a** UV–Vis spectra of PANI in AOT microemulsion synthesized by different water content. **b** UV–Vis spectra of PANI in NMP (1wt%) with different water content AOT microemulsion: **a** W_0=13.9, **b** W_0=27.8, **c** W_0=55.5, and **d** W_0=111.1

Experimental section

Materials

Aniline (99.5%) was distilled twice. Sodium bis(2-ethylhexyl)-sulfosuccinate (AOT, 98%; Aldrich) was used to form micelles in solution. Ammonium peroxydisulfate (APS, 98%) was used to initiate the polymerization. And all other reagents of analytical grade were used as received.

Synthesis of PANI

PANI was synthesized by a mixture of two water-in-oil (W/O) microemulsions, each of which was prepared separately from AOT at a concentration of 0.1 M, heptane, and small amounts of water at various W_0 values (W_0= 13.9, 27.8, 55.5, and 111.1). One microemulsion consists of aniline–HCl aqueous solution (c_{HCl}=1 M), and the other contains APS aqueous solution (1 M). Two microemulsions have the same W_0. The one containing APS aqueous solution was dropwised into the first one with anilinium chloride. The reaction was processed in an ultrasonic disperser at 0 °C. During the process, the colors of mixed microemulsion changed from light blue to dark blue and finally to dark green within 1 h, and then the polymerized microemulsion system was left standing for ca. 24 h. Acetone was then added into the polymerized microemulsion to break emulsion and precipitate the PANI salt. It was filtered and washed with acetone, methanol, ethanol, and finally with deionized water more than five times until

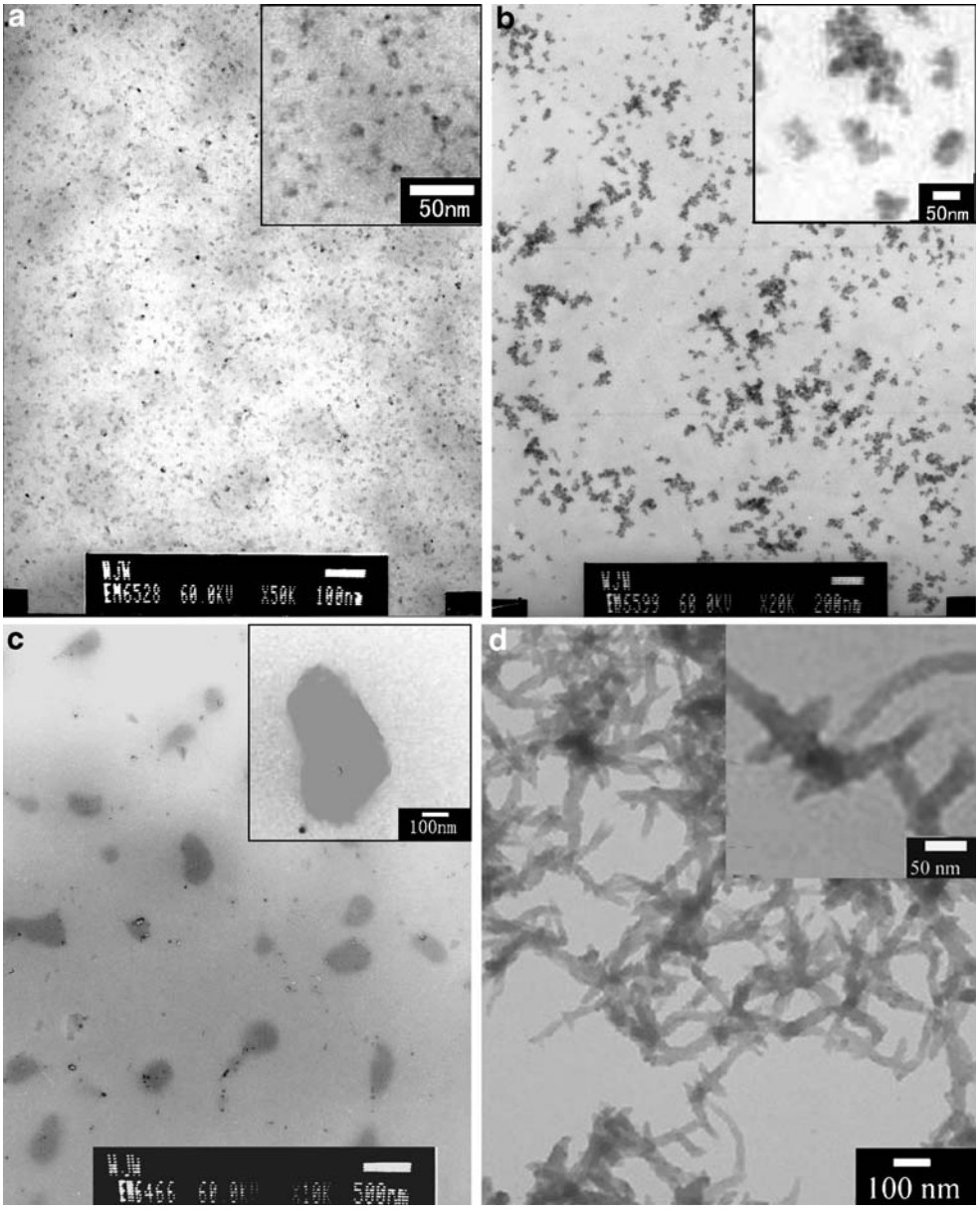

Fig. 4 TEM images of PANI synthesized by different water content AOT microemulsion: **a** W_0=13.9, dispersed nanoparticle (d=10∼20 nm); **b** W_0= 27.8, adherent nanoparticle (d=30∼40 nm); **c** W_0=55.5, lamellar (d=200∼300 nm); and **d** W_0=111.1, dendritic (diameter of 40 nm)

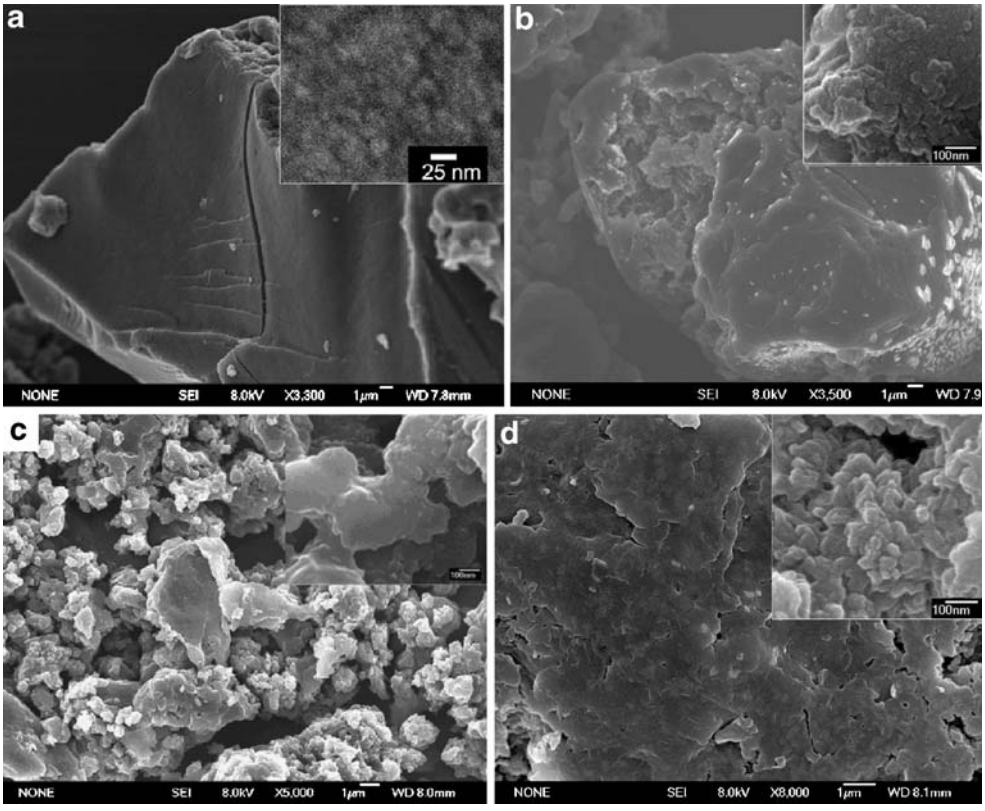

Fig. 5 SEM of PANI synthesized in different water content AOT microemulsion: **a** W_0=13.9, **b** W_0=27.8, **c** W_0=55.5, and **d** W_0=111.1

the filtrate had a pH of 7 when tested by using wet pH paper. The washed product was dried at 60 °C for 12 h in vacuum.

Measurements

The conductivity of microemulsion was measured by a conductometer (model DDS-11A). The morphology of PANI particles formed in micelles was observed with transmission electron microscopy (TEM; JEOL JSM-1200EX). A scanning electron microscopy (SEM; Hitachi H-600) was used to examine the morphology of solid PANI powder. A small amount of powder was fixed on the sample holder using adhesive tape and was coated with a thin layer of gold to improve image resolution. The UV–Visible (UV–Vis) spectra were measured with a TU-1800PC spectrophotometer (Beijing PUXI Instruments). The dispersions were diluted 100 times or more in AOT/heptane solution to achieve a suitable absorbance. Infrared spectroscopy [Fourier transform infrared (FT-IR); Nicolet Magna-750] was used to identify the chemical structure of PANI powder. X-ray diffractometer (RigaKu D/Max-rB) was used with Cu Kα radiation. Conductivities of PANI powder were measured by a four-point probe connected to a Keithley voltmeter-constant current source system.

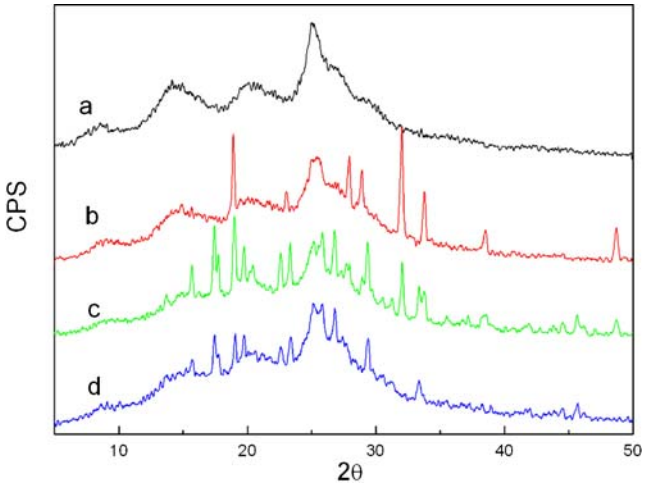

Fig. 6 X-ray diffraction patterns of PANI synthesized in different water content AOT microemulsion: **a** W_0=13.9, **b** W_0=27.8, **c** W_0=55.5, and **d** W_0=111.1

Results and discussion

Microemulsion phases behaviors

An important property of the microemulsion is its capability to solubilize water as microdroplets in a nonpolar phase. So the systems containing the different amount of water show the different phase behaviors and structures. This character can be characterized by electrical conductivity of solution. Among the physicochemical properties of W/O microemulsion, the percolation of conductance is striking

where several folds of increase in conductance takes place after a water content threshold at constant temperature and constant composition [26].

Figure 1 shows the variation of electrical conductivity as a function of water content in AOT reverse microemulsion. As is can be seen in Fig. 1, the conductivity of AOT-formed reverse micelles increases with W_0 at the initial stage. After reaching a maximum, it remains very low until a critical W_0 value when the percolation occurs, followed by a sharp increase with an increase of water content, which suggests that an additional pathway for charge–carrier migration comes into being. When W_0 is small, polymerization takes place within aqueous cores made up of surfactant, and the nanoparticles initially forms in these droplets by a primary growth process. These loaded micellar droplets are in continuous Brownian motion and move erratically and independently in the dispersing oil phase. As the W_0 increases, the interaction and coalescence of droplets also increase [27]. At the percolation stage, the rigidity of the micellar core is greatly reduced upon the addition of water, which leads to the formation of infinite clusters. The addition of a trace amount of water induces one-dimensional growth and the formation of giant flexible cylindrical aggregates. The surfactant aggregates entangle and form a transient network [28].

FT-IR spectra of PANI

The structures of PANI prepared in microemulsion by ultrasonic disperser were studied by FT-IR spectroscopy. The resulting spectra were plotted in transmittance mode as shown in Fig. 2. It can be seen that characteristic peaks of PANI are observed from 3,000 to 500 cm^{-1}. There are no pronounced differences observed, indicating that the main component of each specimen has similar chemical structures. The spectra of PANI with different W_0 are all in good agreement with the previously reported results [8, 16, 29]. In Fig. 2 with the appearance of the 1,565 and 1,480 cm^{-1} modes in both ring deformations, spectra are consistent with quinoid (N=Q=N) and benzenoid (N–B–N), respectively. The bands at 1,128 and 793 cm^{-1} can be attributed to the in-plane and out-of-plane C–H bending modes, and the 1,287 cm^{-1} band can be assigned to C–N stretching of the secondary aromatic amine bending vibration. These results show that all the spectra are similar and consistent with typical PANI, indicating they all have the similar backbone structure of the doped PANI.

UV–Vis spectra of PANI

Figure 3a displays the evolution of absorption spectra of PANI synthesized in different W_0 microemulsion. From Fig. 3a we can see that there exhibits two peaks: an

Table 1 Positions of Bragg's peaks for PANI in different water content $\left(2\theta\{\mathrm{d}(\text{Å})\}\right)^{a}$

Sample																			
a	14.19				20.08			25.04											
b	14.88	15.68		18.94			23.06	25.02	25.46			27.92	28.88		32.02		33.76		38.54	
c	13.74	14.66	15.66	17.44	19.02	19.74	20.40	22.58	23.32	25.16	25.84	26.78	27.72	29.36	30.50	31.30	32.08	33.40	33.74	37.16	38.54	44.62	45.64
d	13.68	14.70	15.70	17.48	19.06	19.76		22.60	23.38	25.18	25.80	26.82		29.36				33.36				44.52	45.64

$\left(2\theta\{\mathrm{d}(\text{Å})\}\right)^{a}$: Bragg's distance d in Å

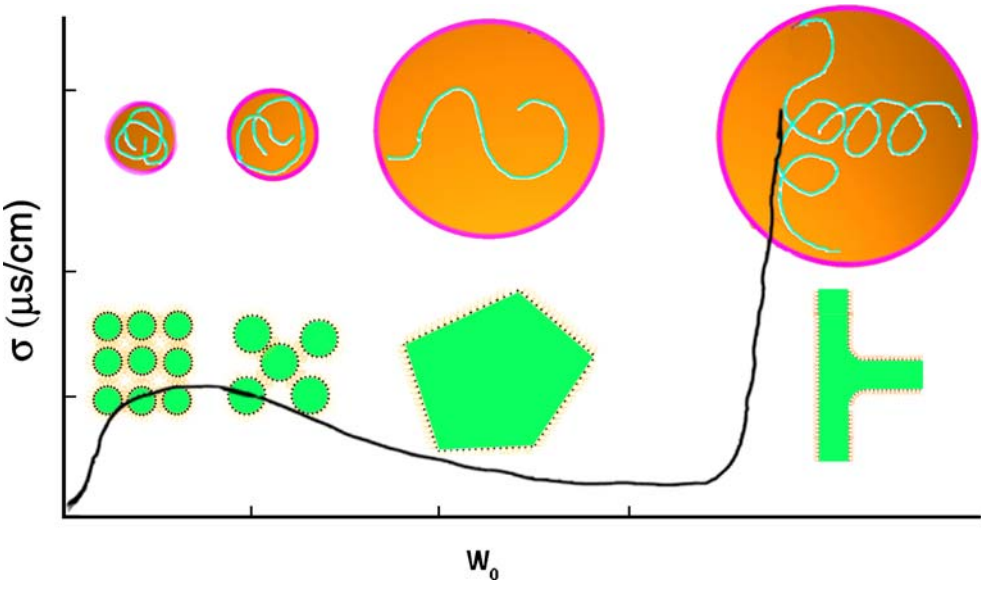

Scheme 1 Schematic diagrams of conductance behaviors with the function of water content

absorption peak at about 400 nm corresponding to the polaron transitions [30] and an absorption peak at about 800 nm, which can be assigned to the $–NH_2^+–$ species, which is generated on doping of the polymer. Fig. 3b shows the UV–Vis spectra of dilute PANI-bases in *N*-methyl pyrrolidone (NMP). For the dilute PANI solution, two major absorption peaks at about 330 nm (π–π* transition of the benzenoid rings) and 633 nm (excitation absorption of the quinoid rings) are observed.

Morphology of PANI

The TEM images showed the morphologies of PANI in the microemulsion system. The inset in Fig. 4 showed the magnified morphology of PANI. They just confirmed that the different water content affected the phase behaviors and finally induced different morphologies.

In the SEM images (Fig. 5), the surfactant was removed so assembly of the polymer took place. In the low water, the polymerization occurred in limited space (microemulsion droplet). When the surfactant is removed PANI nanoparticles can arrange regularly to form a sharp-edged granular morphology because of their small-size effect of nanoparticle. The inset in the Fig. 5a also clearly shows the size of PANI with 10~20 nm. With the increase of W_0, the microemulsion droplets become larger. From the picture we can see that the size of PANI nanoparticles gets to 30~40 nm, and the structure of PANI granular becomes incompact and there is more surface deficiency. As the W_0 was reaching the critical value, coalescence of droplets occurred, and the size of particles increased sharply to 200~300 nm. Because the specific surface area of PANI particles greatly decreased, as they stacked they became more incompact and appeared like powder. Adding water continually induces one-dimensional growth and the formation of giant flexible cylindrical aggregates. The micellar size depends primarily on the molar concentration ratio of the W_0 ($[H_2O]/[AOT]$). Adding water continually can increase the intermicellar exchange of matter between these AOT-inverted micelles. This exchange induces one-dimensional growth and finally the formation of giant flexible cylindrical aggregates through intermicellar collisions. This one-dimensional nanostructure of conducting PANI is called dendritic structure.

X-ray diffraction

The X-ray powder diffraction patterns for the PANI at four different W_0 are presented in Fig. 6. It can be seen that the PANI prepared in W_0=13.9 microemulsion system exhibits two broad bands and one sharp peak at 14, 19, and 26°. As reported in literatures [10, 28, 31], those peaks are characteristic of PANI. However, in the PANI prepared in

Table 2 Effects of different water content on polymerization of aniline

PANI in Different Water Content (W_0)	Conductivity (S cm^{-1})	Shape of PANI in microemulsion	Particle size (nm)	Shape of PANI powder
13.9	0.05	Dispersed nanoparticle	10–20	Sharp-edged granular
27.8	0.11	Adherent nanoparticle	30–40	Defective granular
55.5	2.7	Lamellar	200–300	Powder
111.1	1.8	Dendritic	Diameter of 40	Dendritic

other W_0, there are many sharp peaks in the range of 10~40°. The positions of the main Bragg's peaks and their corresponding d values are summarized in Table 1.

We analyzed this phenomena from the following aspects. First, samples for W_0=13.9 showed that reaction space was too small so that it limited the stretchability of the chains, therefore, it is partly crystalline. Second, the crystallization process includes two stages: the nucleation process and the growth process. In the microemulsions system, droplets can also be called nanoreactor. The aniline monomer is present in nanoreactor and the molecular chains of monomer and oligomer are molecularly oriented by the surfactant in the interface layer of the oil and water phases [9, 32] so the nanoreactor interface can be treated as the nucleus of crystallization. With the increase of W_0, the area of nanoreactor interface increases and the polymer chains have much more space to arrange and polymerize. Subpanels b–d in Fig. 6 exhibit much more diffraction peaks at $2\theta>30°$ than subpanel a (Fig. 6). Third, the increase of water content will induce the increase of aniline concentration in the microemulsion system and the increase of system viscosity. As such, the doped polymer chains are consistent with a progressive change in molecular conformation from "compact coil" to "expanded coil." The increase in aggregation limits the mobility of the chains to allow a crystalline state to be achieved [16, 19]. Fourth, when water content reached 55.5 (Fig. 6c), X-ray diffraction peaks reflect the most ordered state of PANI polymer backbone (the smaller the value of half-width to height, the higher the order). However, as the water content exceeds the critical value, water is in continuous phase and a more open and expanded environment is achieved. So the PANI nanofibers are interconnected to form dendritic structures. Because of its one-dimensional order character, crystallization perfects only on one-dimensional direction and the crystallinity decreased slightly. Based on the above discussion, various W_0 microemulsion system polymerization processes can be clearly described by Scheme 1. In addition, we summarize the morphology and conductivity values of PANI in Table 2.

Conclusions

In summary, high degree of crystallinity and controllable shape conducting PANI were successfully synthesized in the W/O microemulsion by using AOT as the surfactant with different water content ($W_0 = [H_2O]/[AOT]$). During the polymerization, we found that water content has a significant influence on morphology, crystallinity, and conductivity of PANI as the backbone and doped structure is similar.

References

1. MacDiarmid AG, Chiang JC, Halpern M, Huang WS, Mu SL, Somasiri NLD, Wu W, Yaniger SI (1985) Mol Cryst Liq Cryst 121:173–180
2. Chan HSO, Gan LM, Chew CH, Ma L, Seow SH (1993) J Mater Chem 3:1109–1115
3. Mazeikiene R, Malinauskas A (2004) Mater Chem Phys 83:184–192
4. Liu W, Kumar J, Tripathy S (2002) Langmuir 18:9696–9704
5. Thiyagarajan M, Samuelson LA, Kumar J, Cholli AL (2003) J Am Chem Soc 125:11502–11503
6. Marie E, Rothe R, Antonietti M, Landfester K (2003) Macromolecules 36:3967–3973
7. Kim BJ, Oh SG, Han MG, Im SS (2000) Langmuir 16:5841–5845
8. Yan F, Xue G (1999) J Mater Chem 9:3035–3039
9. Osterholm JE, Cao Y, Klavetter F, Smith P (1994) Polymer 35:2902–2906
10. Kim D, Choi J, Kim JY, Han YK, Sohn D (2002) Macromolecules 35:5314–5316
11. Chattopadhyay D, Chakraborty M, Mandal BM (2001) Polym Int 50:538–544
12. Stejskal J, Špírková M, Riede A, Helmstedt M, Mokreva P, Prokeš J (1999) Polymer 40:2487–2492
13. López-Quintela MA, Rivas J (1993) J Colloid Interface Sci 158:446–451
14. Zhou Y, Freitag M, Hone J, Staii C, Johnson AT (2003) Appl Phys Lett 83:3800–3802
15. MacDiarmid AG, Epstein AJ (1995) Synth Met 69:85–92
16. Luzny W, Banka E (2000) Macromolecules 33:425–429
17. McCall RP, Ginder JM, Roe MG, Asturias GE, Scherr EM, Macdiarmid AG, Epstein AJ (1989) Phys Rev B 39:10174–10178
18. Zheng W, Angelopoulos M, Epstein AJ, MacDiarmid AG (1997) Macromolecules 30:2953–2955
19. Li Q, Li T, Wu J (2000) J Phys Chem B 104:9011–9016
20. Li Q, Li T, Wu J (2002) Colloids Surf A Physicochem Eng Asp 197:101–109
21. Andrey JZ, Neville ZM, Anne TH, Jackie YY (2000) Langmuir 16:9168–9176
22. Nave S, Eastoe J (2000) Langmuir 16:8733–8740
23. Pileni MP (1993) J Phys Chem 97:6961–6973
24. Selvan ST, Mani A, Athinarayanasamy K, Phani KLN, Pitchumani S (1995) Mater Res Bull 30:699–705
25. Moulik SP, Dey GC, Bhowmik BB, Panda AK (1999) J Phys Chem B 103:7122–7129
26. Munshi N, De TK, Maitra A (1997) J Colloid Interface Sci 190:387–391
27. Schurtenberger P, Magid LJ, King SM, Lindner P (1991) J Phys Chem 95:4173–4176
28. Rao PS, Sathyanarayana DN, Palaniappan S (2002) Macromolecules 35:4988–4996
29. Tzou K, Gregory RV (1993) Synth Met 53:365–377
30. Liu H, Hu XB, Wang JY, Boughton RI (2002) Macromolecules 35:9414–9419
31. Yan F, Zheng C, Zhai X, Zhao D (1998) J Appl Polym Sci 67:747–754
32. Chen SA, Lee HT (1993) Macromolecules 26:3254–3261